Check for updates

Quantum Chemical and Master Equation Study of OH + CH_2O → H_2O + CHO Reaction Rates in Supercritical CO_2 Environment

Elizabeth E. Wait,[1,2] Artëm E. Masunov,*[1,2,3,4,5] Subith S. Vasu[6]

[1]*NanoScienece Technology Center,* [2]*Department of Chemistry,*
[3]*Department of Physics, University of Central Florida, 12424 Research Parkway, Ste 400, Orlando, FL 32826, USA*
[4] *South Ural State University, Lenin pr. 76, Chelyabinsk 454080, Russia*
[5] *National Research Nuclear University MEPhI, Kashirskoye shosse 31, Moscow, 115409, Russia*
[6] *Center for Advanced Turbomachinery and Energy Research (CATER), Mechanical and Aerospace Engineering, University of Central Florida, Orlando, Florida, 32816, USA*

Abstract. We investigated the reaction rates of OH + CH_2O → H_2O + CHO at CO_2 pressures of up to 1000 atm with and without CO_2 molecule included in reactive complex. Both mechanisms begin with formation of the hydrogen bonded pre-reactive complexes. Our *ab initio* calculations indicate a possibility of catalytic effect, predicting activation barrier that one order of magnitude lower when CO_2 molecule is involved. To verify this effect, we use the Rice-Ramsperger-Kassel-Marcus theory (RRKM) and solve unimolecular master equations in the steady-state approximation. We assume the equilibrium between pre-reactive complexes and reactants and compare the bimolecular reaction rates for the two mechanisms. The catalyzed reaction mechanism is found to be faster at higher CO_2 pressures and lower temperatures, when pre-reactive complexes have non-negligible concentration. Therefore, this catalytic effect may be important for this reactive process in room temperature supercritical CO_2 solvent, but is unlikely to play a role during oxy-combustion.

* To whom correspondence should be addressed, Phone: 1-407-374-3783; E-mail: amasunov@ucf.edu

Author Manuscript

This is the author manuscript accepted for publication and has undergone full peer review but has not been through the copyediting, typesetting, pagination and proofreading process, which may lead to differences between this version and the Version of Record. Please cite this article as doi: 10.1002/kin.21228.

This article is protected by copyright. All rights reserved.

1. Introduction.

In oxy-combustion technology the nitrogen is removed from the air, and oxygen is diluted with excess CO_2.[1] This can prevent the formation of nitrogen oxide pollutants, and simplify carbon sequestration by flue gas separation.[1-2] Another advantage of oxy-combustion is the ability of CO_2 to form a supercritical fluid with high thermal expansion coefficient, increasing the efficiency of the turbine.[3-4] Combustion kinetics may alter at large concentrations of CO_2, and theoretical chemistry can assist in studying these effects.[5-8] In the first paper of this series we investigated the effect of CO_2 on the CO + OH reactive system and found a lower activation energy pathway in which CO_2 participated covalently.[9] In the following papers, we reported lowering of the activation barrier of seven other combustion reactions via van der Waals (vdW) interactions with CO_2.[10,11] In order to obtain a better description of these vdW interactions, we used a higher theory level (CBS-QM11) and refined the reaction pathways.[9, 12] Next, we applied Master Equation solver to obtain rate constants for the $OH + CO \rightarrow H + CO_2$ reaction with and without additional CO_2 molecule.[13]

In this contribution, we investigate the rate of another reaction R1:

$$OH + CH_2O \rightarrow H_2O + CHO \qquad (R1)$$

and focus on the effects of carbon dioxide on the reaction mechanism:

$$OH + CH_2O + [CO_2] \rightarrow H_2O + CHO + [CO_2] \qquad (R2)$$

Formaldehyde CH_2O is formed as intermediate during combustion, and removed by reacting with OH and other radicals. The reaction R1 is very important in combustion chemistry, as was shown by the number of studies.[14-15] Zabarnick *et al.*[16] obtained experimental kinetics data over the temperature range 296-576 K for this reaction using laser photolysis to produce OH from hydrogen peroxide (H_2O_2) and laser-induced fluorescence to measure OH

This article is protected by copyright. All rights reserved.

Author Manuscript

10974601, 2019, 1, Downloaded from https://onlinelibrary.wiley.com/doi/10.1002/kin.21228 by Cochrane Russian Federation, Wiley Online Library on [19/11/2024]. See the Terms and Conditions (https://onlinelibrary.wiley.com/terms-and-conditions) on Wiley Online Library for rules of use; OA articles are governed by the applicable Creative Commons License

concentration. More recently, Sivakumaran *et al.*[17] obtained experimental kinetics data using on-line optical absorption measurements of the formaldehyde concentration at a lower temperature range of 202–399 K, while Vasudevan *et al.*[18] investigated the higher temperature range 934-1670 K using a shock tube with t-C_4H_9OOH and trioxane as the precursors of OH and CH_2O.

Several theoretical studies of reaction R1 had been published as well. Li *et al.*[14] predicted potential energy surface for this reaction using the multicoefficient G3s (MCG3/3) method and found a barrier of 0.21 kcal/mol. They also computed rate constants at 300 to 3000 K using variational transition state theory with small-curvature tunneling correction. Zhao *et al.*[15] reported potential energy surface with a barrier of 5.3 kcal/mol for R1 at MP4(SDTQ)/6-311++G(3df,3pd) theory level. Ali and Barker[19] reported a potential energy surface for R1 reaction using CCSD(T)/aug-cc-pVTZ//CCSD(T)/aug-cc-pVTZ theory level, and found an activation barrier of 3.5 kcal/mol. They also carried out rate calculations at the temperature interval of 200-400 K using canonical transition state theory with Eckart asymmetric tunneling corrections. More recently, Masunov *et al*. also found critical points on the potential energy surface for R1 and one competing reaction at M11/6-311G**+GD3 theory level with zero-point energy (ZPE) correction.[11] They calculated activation barrier to be 4.3 kcal/mol. In this work, we will refine that result using higher theory level CBS-QM11, introduced earlier.[9, 12] Finally, Xu *et al*.[20] predicted R1 reaction rates by fitting the minimum energy pathway to a Morse potential using three different methods. Their Method 1 was CCSD(T)/6-311+G(3df,2p)//CCSD/6-311++G(d,p) theory level and used multiple reflections correction, Method 2 was CCSD(T)/6-311+G(3df,2p)//B3LYP/6-311+G(3df,2p) theory level with multiple reflections, and Method 3 was CCSD(T)/6-311+G(3df,2p)//CCSD/6-311++G(d,p) theory level without multiple reflections. The barrier found using Methods 1

This article is protected by copyright. All rights reserved.

Author Manuscript

10974601, 2019, 1, Downloaded from https://onlinelibrary.wiley.com/doi/10.1002/kin.21228 by Cochrane Russian Federation, Wiley Online Library on [19/11/2024]. See the Terms and Conditions (https://onlinelibrary.wiley.com/terms-and-conditions) on Wiley Online Library for rules of use; OA articles are governed by the applicable Creative Commons License

and 3 was 2.6 kcal/mol, with 2.2 kcal/mol for Method 2. We will consider their results in more details in Section 3. Xu *et al*. accounted for the effect of multiple reflections above the shallow well corresponding to van der Waals (vdW) complexes on the rate of reaction, as was proposed by Hirschfelder and Wigner[21] and formalized by Miller[22]. To account for this effect on the individual rate constant, the probability of the reaction flux passing through was calculated as follows:

$$P_{\mathrm{b}\leftarrow\mathrm{a}} = \frac{P_{\mathrm{b}\leftarrow\mathrm{x}}P_{\mathrm{x}\leftarrow\mathrm{a}}}{P_{\mathrm{b}\leftarrow\mathrm{x}} + P_{\mathrm{a}\leftarrow\mathrm{x}} - P_{\mathrm{b}\leftarrow\mathrm{x}}P_{\mathrm{a}\leftarrow\mathrm{x}}} = \frac{(N_2/N_x)(N_1/N_a)}{(N_2/N_x) + (N_1/N_x) - (N_2/N_x)(N_1/N_x)}$$

Here, the probabilities of vdW complex (x) forming from reactants, this complex decaying back to the reactants (a), and to the products (b) are represented by $P_{\mathrm{x}\leftarrow\mathrm{a}}$, $P_{\mathrm{a}\leftarrow\mathrm{x}}$, and $P_{\mathrm{b}\leftarrow\mathrm{x}}$, respectively, and N_1, N_2, and N_x denote flux integrals through dividing surfaces. In this work we used an alternative approach, where pre-reactive vdW complex (PRC) is assumed to be in equilibrium with reactants, and will show this to be a viable approximation.

First, we calculated accurate activation energies for R1 and R2, based on minimum energy pathway (MEP) described previously at DFT+vdW theory level,[11] and confirmed the additional CO_2 molecule reduces the activation barrier by stabilizing the transition state more than pre-reactive complex. Next, we predicted reaction rate constants for R1 and R2 at a wide range of temperatures and pressures using master equation formalism. Once obtained, these rates are compared in order to find specific conditions where the catalytic effect of CO_2 takes place.

This article is protected by copyright. All rights reserved.

Author Manuscript

10974601, 2019, 1, Downloaded from https://onlinelibrary.wiley.com/doi/10.1002/kin.21228 by Cochrane Russian Federation, Wiley Online Library on [19/11/2024]. See the Terms and Conditions (https://onlinelibrary.wiley.com/terms-and-conditions) on Wiley Online Library for rules of use; OA articles are governed by the applicable Creative Commons License

2. Computational Details.

2.1 Potential Energy Surface.

Gaussian 2009 was used for quantum chemical calculations,[23] and MOLDEN was used to visualize the results.[24] Density Functional Theory (DFT) was shown to be useful in several areas of chemistry,[25-29] providing the best accuracy to computational cost ratio.[30-33] In this work all geometry optimizations and zero point energy (ZPE) calculations were performed using M11 density functional,[34] Grimme's 3-body dispersion correction (GD3),[35] and 6-311G(d,p) basis set.[36] Thereafter, we will call this theory level M11D3. The energies of selected critical points (products, reactants, and transition states) were refined at M11D3 geometries with CBS-M11 model chemistry.[37-38] This composite approach is an improvement over the well-known CBS-QB3.[39] The example of input file for the method CBS-M11 is shown in Supporting Information.

2.2. Rate Constants Calculations.

R1 and R2 both begin via the formation of pre-reactive complexes (PRC) of the initial reagents. The reactions proceed from PRC to the products via unimolecular isomerization. Density of states, equilibrium constants, and microscopic rate coefficients were calculated using TSTRATE, a modified version of the UNIMOL program,[40] included in GPOP program suit.[41] Tunneling effects were taken into account using implementation of asymmetric Eckart potential.[42] SSUMES program suite was used to solve the steady-state unimolecular master equations based on the Rice-Ramsperger-Kassel-Marcus theory (RRKM).[43] The energy grain

This article is protected by copyright. All rights reserved.

Author Manuscript

10974601, 2019, 1, Downloaded from https://onlinelibrary.wiley.com/doi/10.1002/kin.21228 by Cochrane Russian Federation, Wiley Online Library on [19/11/2024]. See the Terms and Conditions (https://onlinelibrary.wiley.com/terms-and-conditions) on Wiley Online Library for rules of use; OA articles are governed by the applicable Creative Commons License

size used was set to default value of 100 cm^{-1}, which typically gives converged results for combustion reactions.[44] Collisional energy transfer probability was estimated using exponential-down model.[45] Collision frequency was estimated by assuming the Lennard-Jones (LJ) potential. The LJ parameters for R1 reactive system were taken to be identical to those of CO_2 (σ = 3.94 Å and ε/k_B = 201 K). This choice was determined by the fact that CO_2 and PC28 contain three heavy atoms in linear or nearly linear configuration. For R2 reactive system we used LJ parameters equal to that of benzene (σ = 4.70 Å and ε/k_B = 284 K). Both C_6H_6 and PC128 contain six heavy atoms in the planar or nearly planar hexagonal arrangement. This collision model was used to successfully describe pressure dependence on reactive system of a similar size in the past.[13] The buffer gas used was CO_2 in both cases. The pressure dependent rate constants were calculated by solving the energy grained, multiple-well master equation for the reactions R1 and R2. The truncation threshold was set to 50 energy grains. Moderate variations (5-100) in this truncation threshold did not have a sizable effect on the outcome.

3. Results and Discussion.

3.1 OH + CH_2O Reactive System.

As shown in Fig. 1, reaction R1 begins with formation of hydrogen bonded pre-reactive complex PRC28 (-2.9 kcal/mol below the initial reactants). This complex is formed with no barrier and is presumed be in equilibrium with the reactants.

$$OH + CH_2O \leftrightarrow PRC28 \quad (R3)$$

PRC28 isomerizes to the product complex PC28 over TS28 with 3.04 kcal/mol barrier:

$$PRC28 \rightarrow [TS28] \rightarrow PC28 \quad (R4)$$

This article is protected by copyright. All rights reserved.

Author Manuscript

10974601, 2019, 1, Downloaded from https://onlinelibrary.wiley.com/doi/10.1002/kin.21228 by Cochrane Russian Federation, Wiley Online Library on [19/11/2024]. See the Terms and Conditions (https://onlinelibrary.wiley.com/terms-and-conditions) on Wiley Online Library for rules of use; OA articles are governed by the applicable Creative Commons License

The product complex can then (1) dissociate into the products:

$$PC28 \rightarrow H_2O + CHO \quad (R5)$$

or (3) isomerize back to PRC28 via TS28.

$$PC28 \rightarrow [TS28] \rightarrow PRC28 \quad (R6)$$

The equilibrium constant for PRC28 formation (R3) can be defined as follows:

$$K_{PRC28} = [PRC28] / [OH]\,[CH_2O] \quad (1)$$

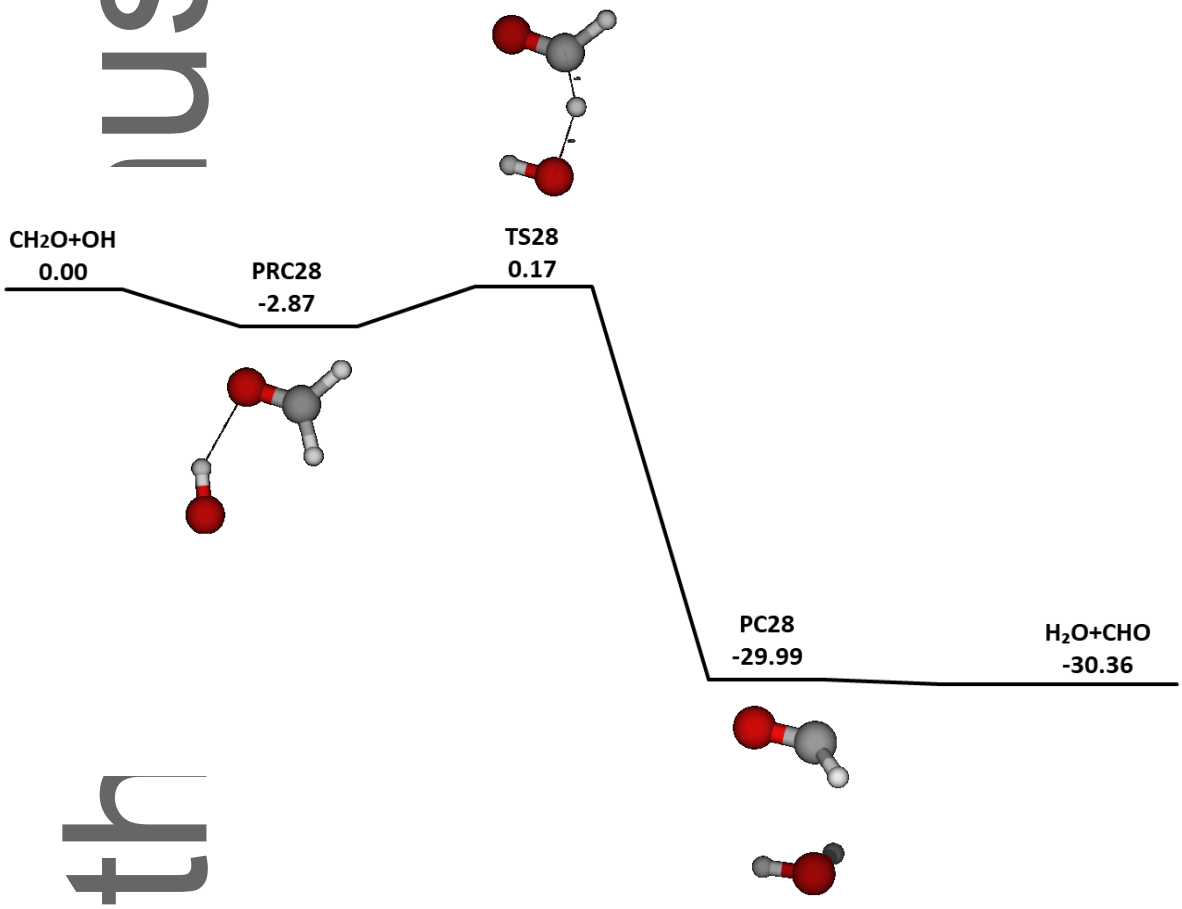

Figure 1. CBS-QM11 potential energy surface for reaction R1 (ZPE included).

The equilibrium constant for PRC formation as well as the high-pressure limit for the R4 (TS28 unimolecular rate k_{28}^{∞}) was computed as a function of T. Next, the pressure

This article is protected by copyright. All rights reserved.

10974601, 2019, 1, Downloaded from https://onlinelibrary.wiley.com/doi/10.1002/kin.21228 by Cochrane Russian Federation, Wiley Online Library on [19/11/2024]. See the Terms and Conditions (https://onlinelibrary.wiley.com/terms-and-conditions) on Wiley Online Library for rules of use; OA articles are governed by the applicable Creative Commons License

dependence was taken into account by means of branching fractions for all the intermediates in steady state approximation. The unimolecular rate coefficient k_{28} was calculated by multiplying k_{28}^{∞} and the forward reaction branching fraction. The rate for reaction R1 is

$$\text{rate R1} = k_1\,[\text{OH}][\text{CH}_2\text{O}] = k_{28}\,[\text{PRC28}] \qquad (2)$$

and bimolecular rate constant was therefore obtained as

$$k_1 = k_{28}\,\text{K}_{\text{PRC}} \qquad (3)$$

The calculated temperature dependence is compared to theoretical and experimental data in **Fig. 2**.

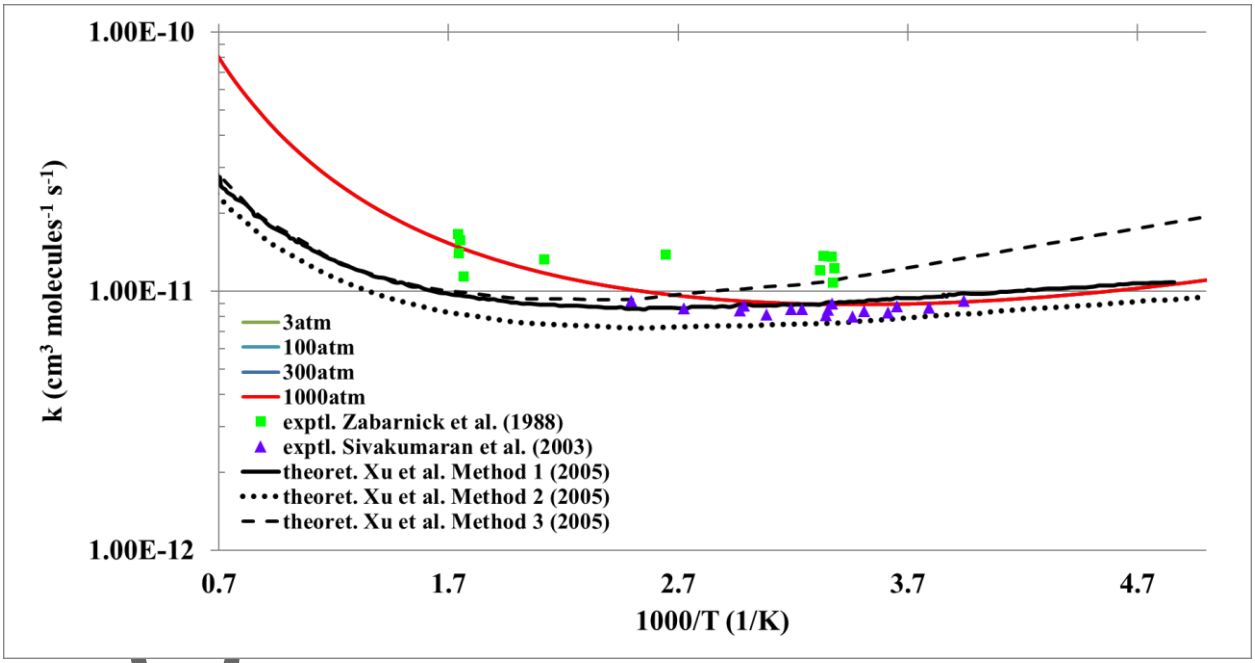

Figure 2. Bimolecular rate constants for reaction R1, calculated at 3, 100, 300, and 1000 atm. All pressure sets are plotted, but overlap. The experimental data are shown for comparison (green squares from Ref.[16], purple triangles from Ref.[17]). Black lines illustrate predictions from Ref.[20] See text for details.

One can see from **Fig.2**, that predicted rate constants agree well with experimental data. The predicted trend is consistent with that of Xu *et al.*[20] at lower temperatures. Our results are in better agreement with the Methods 1 and 2, that include correction for multiple reflections above potential well of pre-reactive complex. This indicates that our approach is a

This article is protected by copyright. All rights reserved.

Author Manuscript

10974601, 2019, 1, Downloaded from https://onlinelibrary.wiley.com/doi/10.1002/kin.21228 by Cochrane Russian Federation, Wiley Online Library on [19/11/2024]. See the Terms and Conditions (https://onlinelibrary.wiley.com/terms-and-conditions) on Wiley Online Library for rules of use; OA articles are governed by the applicable Creative Commons License

viable alternative for multiple reflection correction to the rate constant of a bimolecular reaction. Deviations of the Method 3 are consistent with conclusions by Hirschfelder and Wigner,[21] who argued this effect is only important at low temperatures. It is worth noting that reaction **R1** is found not to be pressure dependent.

3.2 OH + CH_2O Reactive System with CO_2.

Previously, we found two possible mechanisms for **R2** reaction:[11] one included several steps with the extra CO_2 molecule covalently bound in the transition states and intermediates, and the other one involved a hydrogen transfer from CH_2O to OH to form water, with TS stabilized by vdW complex formation with extra CO_2 molecule. The activation barrier for former mechanism was found to be 30.2 kcal/mol at M11D3+ZPE, whereas the barrier for the latter was found to be 0.8 kcal/mol. Therefore, we will only consider the second mechanism here.

Author Manuscript

This article is protected by copyright. All rights reserved.

10974601, 2019, 1, Downloaded from https://onlinelibrary.wiley.com/doi/10.1002/kin.21228 by Cochrane Russian Federation, Wiley Online Library on [19/11/2024]. See the Terms and Conditions (https://onlinelibrary.wiley.com/terms-and-conditions) on Wiley Online Library for rules of use; OA articles are governed by the applicable Creative Commons License

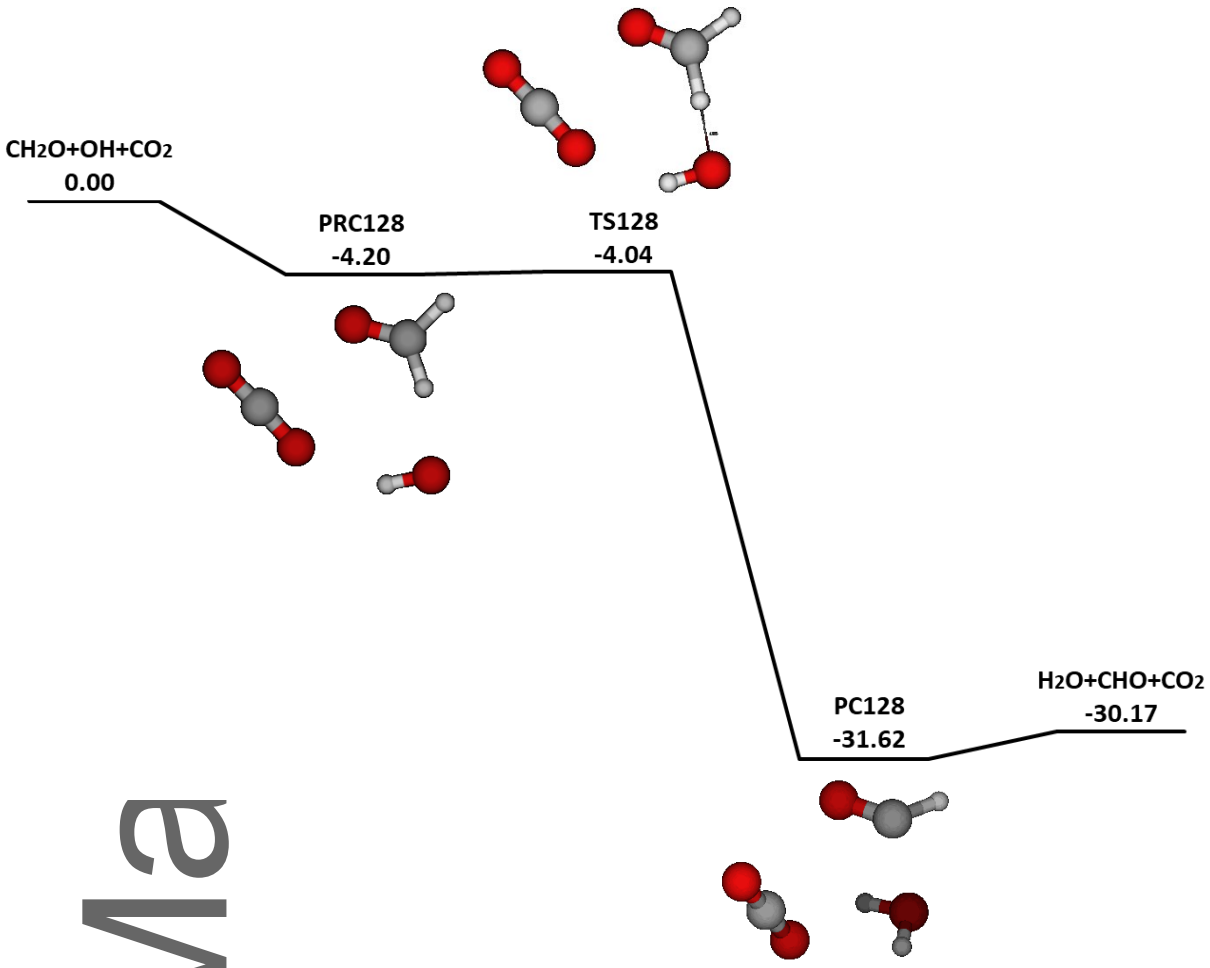

Figure 3. CBS-QM11 potential energy surface for reaction R2 (ZPE included).

The mechanism involving spectator CO_2 is illustrated in **Fig. 3** and can be summarized as follows. First, pre-reactive complex PRC128 (-4.2 kcal/mol) is formed:

$$CH_2O + OH + CO_2 \leftrightarrow PRC128 \quad (R7)$$

PRC128 and the reactants are again assumed to be in equilibrium. This complex then isomerizes via TS128 with 0.16 kcal/mol barrier into the product complex:

$$PRC128 \rightarrow [TS128] \rightarrow PC128 \quad (R8)$$

The product complex PC128 can then dissociate into products:

This article is protected by copyright. All rights reserved.

Author Ma

10974601, 2019, 1, Downloaded from https://onlinelibrary.wiley.com/doi/10.1002/kin.21228 by Cochrane Russian Federation, Wiley Online Library on [19/11/2024]. See the Terms and Conditions (https://onlinelibrary.wiley.com/terms-and-conditions) on Wiley Online Library for rules of use; OA articles are governed by the applicable Creative Commons License

$$PC128 \rightarrow CHO + H_2O + CO_2 \quad (R9)$$

or isomerize back to PRC128:

$$PC128 \rightarrow [TS128] \rightarrow PRC128 \quad (R10)$$

The activation barrier for R2 is lower than that of R1, due to the fact that vdW complex formation stabilizes the transition state more than it does for PRC. The high-pressure limit for unimolecular rate constant k_{128}^{∞} and the equilibrium constant for PRC formation K_{PRC128} were found as functions of T. Equilibrium constant for PRC formation K_{PRC128} is defined as:

$$K_{PRC128} = [PRC128] / [OH]\,[CH_2O]\,[CO_2] \quad (4)$$

The pressure dependent constant k_{128} was calculated by multiplying k_{128}^{∞} with the forward reaction branching fraction. The rate for the overall reaction R2 is:

$$\text{rate R2} = k_2\,[OH]\,[CH_2O] = k_{128}\,[PRC128] \quad (5)$$

so that bimolecular rate constant k_2 can be expressed as:

$$k_2 = k_{128}\,K_{PRC128}\,[CO_2] \quad (6)$$

Concentration of CO_2 was obtained from the pressure and temperature using NIST database of real gases.[46] The bimolecular rate constant k_2 was calculated in this procedure for several pressure levels and plotted in **Fig. 4** together with k_1. From this figure one can see that R2 rate exceeds R1 rate only at higher pressures and lower temperatures (below 313K at 1000 atm and below 303K at 300 atm). Apparently, at these conditions ternary pre-reactive complex is present in sufficient concentrations for the catalytic mechanism to compete. Similar conclusions were made when considering the catalysis of atmospheric reactions by the water molecules.[47-48]

This article is protected by copyright. All rights reserved.

Author Manuscript

10974601, 2019, 1, Downloaded from https://onlinelibrary.wiley.com/doi/10.1002/kin.21228 by Cochrane Russian Federation, Wiley Online Library on [19/11/2024]. See the Terms and Conditions (https://onlinelibrary.wiley.com/terms-and-conditions) on Wiley Online Library for rules of use; OA articles are governed by the applicable Creative Commons License

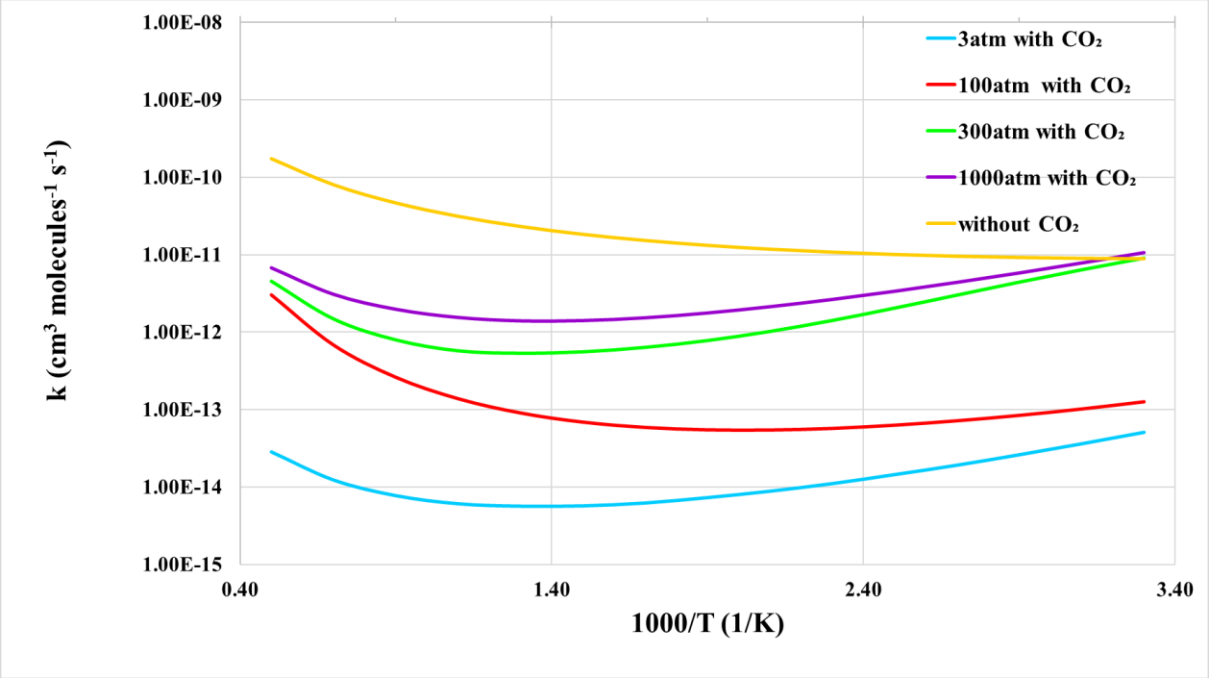

Figure 4. Bimolecular rate constants, calculated at a range of temperatures for reactions R1 (without CO_2) and R2 (with CO_2).

4. Conclusions

We found potential energy surface for OH + CH_2O → H_2O + CHO reaction with (R2) and without (R1) additional CO_2 molecule using *ab initio* CBS-QM11 theory level. The activation barrier without CO_2 present was 3.04 kcal/mol, but with CO_2 it was lowered to 0.16 kcal/mol. Based on this reduction in activation barrier, we suggested a catalytic effect of CO_2 on this important combustion reaction is possible. We then predicted rate constants for R1 and R2 in a supercritical CO_2 environment. Investigation of the reaction mechanisms was carried out using the steady-state master equation analyses based on the Rice-Ramsperger-Kassel-Marcus theory. We found that at higher CO_2 pressures (300 atm) and lower temperatures (below 313 K) the reaction R2 becomes faster than reaction R1, due to the fact that pre-reactive complexes are present at sufficient concentrations. These findings are consistent with our previous work on autocatalytic effects in the OH + CO → H + CO_2

This article is protected by copyright. All rights reserved.

Author Manuscript

10974601, 2019, 1, Downloaded from https://onlinelibrary.wiley.com/doi/10.1002/kin.21228 by Cochrane Russian Federation, Wiley Online Library on [19/11/2024]. See the Terms and Conditions (https://onlinelibrary.wiley.com/terms-and-conditions) on Wiley Online Library for rules of use; OA articles are governed by the applicable Creative Commons License

reaction.[13] The effect of carbon dioxide on $OH+CH_2O$ reaction would be important in liquid CO_2 at room temperature, but not for oxy-combustion processes.

Acknowledgments

This work was supported in part by the Department of Energy (grant number: DE-FE0025260). The authors acknowledge the National Energy Research Scientific Computing Center (NERSC), and the University of Central Florida Advanced Research Computing Center (https://arcc.ist.ucf.edu) for providing computational resources and support. A.E.M. gratefully acknowledges support from the Act 211 by Government of the Russian Federation (Contract No. 02.A03.21.0011) and by the "improving of the competitiveness" program of the National Research Nuclear University MEPhI. E.E.W. is grateful for the support of the UCF Research and Mentoring Program (RAMP), Office of Research and Commercialization (ORC), and the Office of Undergraduate Research (OUR). Disclaimer: This report was prepared as an account of work sponsored by an agency of the United States Government. Neither the United States Government nor any agency thereof, nor any of their employees, makes any warranty, express or implied, or assumes any legal liability or responsibility for the accuracy, completeness, or usefulness of any information, apparatus, product, or process disclosed, or represents that its use would not infringe privately owned rights. Reference herein to any specific commercial product, process, or service by trade name, trademark, manufacturer, or otherwise does not necessarily constitute or imply its endorsement, recommendation, or favoring by the United States Government or any agency thereof. The views and opinions of authors expressed herein do not necessarily state or reflect those of the United States Government or any agency thereof.

This article is protected by copyright. All rights reserved.

Author Manuscript

10974601, 2019, 1, Downloaded from https://onlinelibrary.wiley.com/doi/10.1002/kin.21228 by Cochrane Russian Federation, Wiley Online Library on [19/11/2024]. See the Terms and Conditions (https://onlinelibrary.wiley.com/terms-and-conditions) on Wiley Online Library for rules of use; OA articles are governed by the applicable Creative Commons License

References

1. Bongartz, D.; Ghoniem, A. F., Chemical Kinetics Mechanism for Oxy-Fuel Combustion of Mixtures of Hydrogen Sulfide and Methane. *Combustion and Flame* **2015**, *162*, 544-553.
2. Tan, Y.; Douglas, M. A.; Thambimuthu, K. V., Co2 Capture Using Oxygen Enhanced Combustion Strategies for Natural Gas Power Plants. *Fuel* **2002**, *81*, 1007-1016.
3. Utamura, M.; Hasuike, H.; Yamamoto, T., Demonstration Test Plant of Closed Cycle Gas Turbine with Supercritical Co2 as Working Fluid. *Strojarstvo* **2010**, *52*, 459-465.
4. Zhang, X. R.; Yamaguchi, H.; Fujima, K.; Enomoto, M.; Sawada, N., Theoretical Analysis of a Thermodynamic Cycle for Power and Heat Production Using Supercritical Carbon Dioxide. *Energy* **2007**, *32*, 591-599.
5. Gadzhiev, O. B.; Ignatov, S. K.; Razuvaev, A. G.; Masunov, A. E., Quantum Chemical Study of Trimolecular Reaction Mechanism between Nitric Oxide and Oxygen in the Gas Phase. *Journal of Physical Chemistry A* **2009**, *113*, 9092-9101.
6. Gadzhiev, O. B.; Ignatov, S. K.; Gangopadhyay, S.; Masunov, A. E.; Petrov, A. I., Mechanism of Nitric Oxide Oxidation Reaction (2no+O-2 -> 2no(2)) Revisited. *Journal of Chemical Theory and Computation* **2011**, *7*, 2021-2024.
7. Gadzhiev, O. B.; Ignatov, S. K.; Krisyuk, B. E.; Maiorov, A. V.; Gangopadhyay, S.; Masunov, A. E., Quantum Chemical Study of the Initial Step of Ozone Addition to the Double Bond of Ethylene. *Journal of Physical Chemistry A* **2012**, *116*, 10420-10434.
8. Ignatov, S. K.; Gadzhiev, O. B.; Razuvaev, A. G.; Masunov, A. E.; Schrems, O., Adsorption of Glyoxal (Chocho) and Its Uv Photolysis Products on the Surface of Atmospheric Ice Nanoparticles. Dft and Density Functional Tight-Binding Study. *Journal of Physical Chemistry C* **2014**, *118*, 7398-7413.
9. Masunov, A. E.; Wait, E.; Vasu, S. S., Chemical Reaction Co+Oh -> Co2+H Autocatalyzed by Carbon Dioxide: Quantum Chemical Study of the Potential Energy Surfaces. *Journal of Physical Chemistry A* **2016**, *120*, 6023-6028.
10. Masunov, A. E.; Atlanov, A. A.; Vasu, S. S., Potential Energy Surfaces for the Reactions of Ho2 Radical with Ch2o and Ho2 in Co2 Environment. *The Journal of Physical Chemistry A* **2016**, *120*, 7681-7688.
11. Masunov, A. E.; Wait, E.; Vasu, S. S., Quantum Chemical Study of Ch3 + O-2 Combustion Reaction System: Catalytic Effects of Additional Co2 Molecule. *Journal of Physical Chemistry A* **2017**, *121*, 5681-5689.
12. Masunov, A. E.; Wait, E. E.; Atlanov, A. A.; Vasu, S. S., Quantum Chemical Study of Supercritical Carbon Dioxide Effects on Combustion Kinetics. *The Journal of Physical Chemistry A* **2017**, *121*, 3728-3735.
13. Masunov, A. E.; Wait, E.; Vasu, S. S., Catalytic Effect of Carbon Dioxide on Reaction Oh+Co→H+Co2 in Supercritical Environment: Master Equation Study. *Journal of Physical Chemistry* **2018**, *ASAP*, http://dx.doi.org/10.1021/acs.jpca.8b04501.
14. Li, H.-Y.; Pu, M.; Ji, Y.-Q.; Xu, Z.-F.; Feng, W.-L., Theoretical Study on the Reaction Path and Rate Constants of the Hydrogen Atom Abstraction Reaction of Ch2o with Ch3/Oh. *Chemical Physics* **2004**, *307*, 35-43.
15. Zhao, Y.; Wang, B.; Li, H.; Wang, L., Theoretical Studies on the Reactions of Formaldehyde with Oh and Oh−. *Journal of Molecular Structure: THEOCHEM* **2007**, *818*, 155-161.
16. Zabarnick, S.; Fleming, J. W.; Lin, M. C., Kinetics of Hydroxyl Radical Reactions with Formaldehyde and 1,3,5-Trioxane between 290 and 600 K. *International Journal of Chemical Kinetics* **1988**, *20*, 117-129.
17. Sivakumaran, V.; Hölscher, D.; Dillon, T. J.; Crowley, J. N., Reaction between Oh and Hcho: Temperature Dependent Rate Coefficients (202–399 K) and Product Pathways (298 K). *Physical Chemistry Chemical Physics* **2003**, *5*, 4821-4827.

This article is protected by copyright. All rights reserved.

Author Manuscript

10974601, 2019, 1, Downloaded from https://onlinelibrary.wiley.com/doi/10.1002/kin.21228 by Cochrane Russian Federation, Wiley Online Library on [19/11/2024]. See the Terms and Conditions (https://onlinelibrary.wiley.com/terms-and-conditions) on Wiley Online Library for rules of use; OA articles are governed by the applicable Creative Commons License

18. Vasudevan, V.; Davidson, D. F.; Hanson, R. K., Direct Measurements of the Reaction Oh + Ch2o → Hco + H2o at High Temperatures. *International Journal of Chemical Kinetics* **2005**, *37*, 98-109.
19. Akbar Ali, M.; Barker, J. R., Comparison of Three Isoelectronic Multiple-Well Reaction Systems: Oh + Ch2o, Oh + Ch2ch2, and Oh + Ch2nh. *The Journal of Physical Chemistry A* **2015**, *119*, 7578-7592.
20. Xu, S.; Zhu, R. S.; Lin, M. C., Ab Initio Study of the Oh + Ch2o Reaction: The Effect of the Oh··Och2 Complex on the H-Abstraction Kinetics. *International Journal of Chemical Kinetics* **2006**, *38*, 322-326.
21. Hirschfelder, J. O.; Wigner, E. P., Some Quantum-Mechanical Considerations in the Theory of Reactions Involving an Activation Energy. In *Part I: Physical Chemistry. Part Ii: Solid State Physics*, Wightman, A. S., Ed. Springer Berlin Heidelberg: Berlin, Heidelberg, 1997; pp 176-188.
22. Miller, W. H., Unified Statistical Model for ''Complex'' and ''Direct'' Reaction Mechanisms. *The Journal of Chemical Physics* **1976**, *65*, 2216-2223.
23. Frisch, M. J., et al. *Gaussian 09, Rev. D.01*, Gaussian, Inc.: Wallingford CT, 2009.
24. Schaftenaar, G.; Noordik, J. H., Molden: A Pre- and Post-Processing Program for Molecular and Electronic Structures. *Journal of Computer-Aided Molecular Design* **2000**, *14*, 123-134.
25. Suponitsky, K. Y.; Masunov, A. E., Supramolecular Step in Design of Nonlinear Optical Materials: Effect of Pi ... Pi Stacking Aggregation on Hyperpolarizability. *Journal of Chemical Physics* **2013**, *139*, 094310.
26. Belfield, K. D.; Bondar, M. V.; Frazer, A.; Morales, A. R.; Kachkovsky, O. D.; Mikhailov, I. A.; Masunov, A. E.; Przhonska, O. V., Fluorene-Based Metal-Ion Sensing Probe with High Sensitivity to Zn2+ and Efficient Two-Photon Absorption. *J. Phys. Chem. B* **2010**, *114*, 9313-9321.
27. Mikhailov, I. A.; Bondar, M. V.; Belfield, K. D.; Masunov, A. E., Electronic Properties of a New Two-Photon Absorbing Fluorene Derivative: The Role of Hartree-Fock Exchange in the Density Functional Theory Design of Improved Nonlinear Chromophores. *Journal of Physical Chemistry C* **2009**, *113*, 20719-20724.
28. Belfield, K. D.; Bondar, M. V.; Hernandez, F. E.; Masunov, A. E.; Mikhailov, I. A.; Morales, A. R.; Przhonska, O. V.; Yao, S., Two-Photon Absorption Properties of New Fluorene-Based Singlet Oxygen Photosensitizers. *Journal of Physical Chemistry C* **2009**, *113*, 4706-4711.
29. De Boni, L.; Toro, C.; Masunov, A. E.; Hernandez, F. E., Untangling the Excited States of Dr1 in Solution: An Experimental and Theoretical Study. *Journal of Physical Chemistry A* **2008**, *112*, 3886-3890.
30. Masunov, A.; Tretiak, S.; Hong, J. W.; Liu, B.; Bazan, G. C., Theoretical Study of the Effects of Solvent Environment on Photophysical Properties and Electronic Structure of Paracyclophane Chromophores. *Journal of Chemical Physics* **2005**, *122*.
31. Kobko, N.; Masunov, A.; Tretiak, S., Calculations of the Third-Order Nonlinear Optical Responses in Push-Pull Chromophores with a Time-Dependent Density Functional Theory. *Chemical Physics Letters* **2004**, *392*, 444-451.
32. Cardenas-Jiron, G. I.; Masunov, A.; Dannenberg, J. J., Molecular Orbital Study of Crystalline P-Benzoquinone. *Journal of Physical Chemistry A* **1999**, *103*, 7042-7046.
33. Masunov, A. E.; Zorkii, P. M., Geometric Characteristics of Halogen-Halogen Intermolecular Contacts in Organic-Crystals *Zhurnal Fizicheskoi Khimii* **1992**, *66*, 60-69.
34. Peverati, R.; Truhlar, D. G., Improving the Accuracy of Hybrid Meta-Gga Density Functionals by Range Separation. *Journal of Physical Chemistry Letters* **2011**, *2*, 2810-2817.
35. McLean, A. D.; Chandler, G. S., Contracted Gaussian-Basis Sets for Molecular Calculations .1. 2nd Row Atoms, Z=11-18. *Journal of Chemical Physics* **1980**, *72*, 5639-5648.

This article is protected by copyright. All rights reserved.

Author Manuscript

10974601, 2019, 1, Downloaded from https://onlinelibrary.wiley.com/doi/10.1002/kin.21228 by Cochrane Russian Federation, Wiley Online Library on [19/11/2024]. See the Terms and Conditions (https://onlinelibrary.wiley.com/terms-and-conditions) on Wiley Online Library for rules of use; OA articles are governed by the applicable Creative Commons License

36. Grimme, S.; Antony, J.; Ehrlich, S.; Krieg, H., A Consistent and Accurate Ab Initio Parametrization of Density Functional Dispersion Correction (Dft-D) for the 94 Elements H-Pu. *Journal of Chemical Physics* **2010**, *132*.
37. Montgomery, J. A.; Frisch, M. J.; Ochterski, J. W.; Petersson, G. A., A Complete Basis Set Model Chemistry. Vi. Use of Density Functional Geometries and Frequencies. *Journal of Chemical Physics* **1999**, *110*, 2822-2827.
38. Montgomery, J. A.; Frisch, M. J.; Ochterski, J. W.; Petersson, G. A., A Complete Basis Set Model Chemistry. Vii. Use of the Minimum Population Localization Method. *Journal of Chemical Physics* **2000**, *112*, 6532-6542.
39. Peterson, K. A.; Feller, D.; Dixon, D. A., Chemical Accuracy in Ab Initio Thermochemistry and Spectroscopy: Current Strategies and Future Challenges. *Theoretical Chemistry Accounts* **2012**, *131*.
40. Gilbert, R. S., S.; Jordan, M. *Unimol Program Suite*, available from the authors: School of Chemistry, Sydney University, NSW 2006, Australia, 1993.
41. Miyoshi, A. *Gpop Program*, http://www.frad.t.u-tokyo.ac.jp/~miyoshi/gpop/.
42. Garrett, B. C.; Truhlar, D. G., Semiclassical Tunneling Calculations. *The Journal of Physical Chemistry* **1979**, *83*, 2921-2926.
43. Miyoshi, A. *Ssumes Program*, http://www.frad.t.u-tokyo.ac.jp/~miyoshi/ssumes/.
44. Matsugi, A.; Suma, K.; Miyoshi, A., Kinetics and Mechanisms of the Allyl Plus Allyl and Allyl Plus Propargyl Recombination Reactions. *Journal of Physical Chemistry A* **2011**, *115*, 7610-7624.
45. Matsugi, A., Collision Frequency for Energy Transfer in Unimolecular Reactions. *The Journal of Physical Chemistry A* **2018**, *122*, 1972-1985.
46. Lemmon, E. W.; McLinden, M. O.; Friend, D. G., Thermophysical Properties of Fluid Systems. In *Nist Chemistry Webbook, Nist Standard Reference Database Number 69*, National Institute of Standards and Technology, Gaithersburg MD, 20899.
47. Zhang, W.; Du, B.; Qin, Z., Catalytic Effect of Water, Formic Acid, or Sulfuric Acid on the Reaction of Formaldehyde with Oh Radicals. *The Journal of Physical Chemistry A* **2014**, *118*, 4797-4807.
48. Iuga, C.; Alvarez-Idaboy, J. R.; Reyes, L.; Vivier-Bunge, A., Can a Single Water Molecule Really Catalyze the Acetaldehyde + Oh Reaction in Tropospheric Conditions? *The Journal of Physical Chemistry Letters* **2010**, *1*, 3112-3115.

Author Manuscript

This article is protected by copyright. All rights reserved.

10974601, 2019, 1, Downloaded from https://onlinelibrary.wiley.com/doi/10.1002/kin.21228 by Cochrane Russian Federation, Wiley Online Library on [19/11/2024]. See the Terms and Conditions (https://onlinelibrary.wiley.com/terms-and-conditions) on Wiley Online Library for rules of use; OA articles are governed by the applicable Creative Commons License